SARS-CoV-2 Infection of Salivary Glands Predisposes to Oral Candidiasis

Areej Alfaifi[1,2,3], Tristan Wang[1], Paola Perez [4], Ahmed S. Sultan[1,5], Timothy F. Meiller[1,5], Peter Rock[6], David E. Kleiner[7], Daniel S. Chertow[8,9], Stephen M. Hewitt[7], Billel Gasmi[7], Sydney Stein[8], Sabrina Ramelli[8], Daniel Martin[10], Blake M. Warner*[4], Mary Ann Jabra-Rizk*[1,11]

Affiliations:

[1] Department of Oncology and Diagnostic Sciences, School of Dentistry, University of Maryland Baltimore, USA
[2] Department of Restorative and Prosthetic Dental Sciences, College of Dentistry, King Saud bin Abdulaziz University for Health Sciences, Riyadh, Saudi Arabia
[3] King Abdullah International Medical Research Center (KAIMRC), Riyadh, Saudi Arabia
[4] Salivary Disorders Unit, National Institute of Dental and Craniofacial Research, National Institutes of Health, Bethesda, MD, USA
[5] University of Maryland Greenebaum Cancer Center, Baltimore, MD, USA
[6] Department of Anesthesia, School of Medicine, University of Maryland, Baltimore, MD 21201, USA
[7] Laboratory of Pathology, Center for Cancer Research, National Cancer Institute, National Institutes of Health, Bethesda, Maryland
[8] Critical Care Medicine Department, Clinical Center, National Institutes of Health, Bethesda, MD, USA
[9] Laboratory of Virology, National Institute of Allergy and Infectious Diseases, National Institutes of Health, Hamilton, MT, USA
[10] Genomics and Computational Biology Core, National Institute of Dental and Craniofacial Research, National Institutes of Health, Bethesda, MD, USA
[11] Department of Microbiology and Immunology, School of Medicine, University of Maryland, Baltimore, MD 21201, USA

**** Co-Corresponding Authors***

To Whom Correspondence Should Be Addressed:

Mary Ann Jabra-Rizk, PhD
Address: 650 W. Baltimore St., 7th Floor, Baltimore, MD 21201
Telephone number: +1 (410)-706-0508
E-mail address: mrizk@umaryland.edu

Blake M. Warner, DDS, PhD, MPH
Address: Building 10, Room 1A01, 10 Center Drive, Bethesda, MD, 20895
Telephone number: +1 (301)-500-8063
E-mail address: blake.warner@nih.gov

ABSTRACT

SARS-CoV-2 targets salivary glands potentially impacting oral health. We show that presence of replicating viruses in the acinar cells of salivary glands compromises production and secretion of histatin-5, a key host-produced antifungal peptide. The salivary levels of histatin-5 were significantly reduced in SARS-CoV-2 infected subjects, concomitant with enhanced prevalence of the fungal opportunistic pathogen *Candida albicans*. These findings provide direct evidence associating SARS-CoV-2 infection with predisposition to oral candidiasis.

The oral cavity remains an underappreciated site for SARS-CoV-2 infection despite the myriad of oral conditions reported in COVID-19 patients[1]. The homeostasis of the oral cavity is maintained by saliva, extracellular fluid produced by salivary glands possessing a wealth of protective properties[2]. Specifically, saliva is enriched with antimicrobial peptides that play a vital role in innate immune defenses against microbial species[2]. Most notable are histatins, a family of peptides exclusively produced in the acinar cells of the salivary glands and secreted into saliva[3]. Histatin-5 specifically is the most abundant and unique as it exhibits potent antifungal activity against the fungal pathogen *Candida albicans*[4,5]. Although *C. albicans* is a commensal colonizer of the oral cavity, any changes in the host microenvironment favoring its proliferation allows this opportunistic species to transition into a pathogen causing oral candidiasis (thrush)[6,7]. Local oral innate immune defenses, and specifically histatin-5, are hypothesized to maintain *Candida* in its commensal state[8].

Huang & Perez[9] comprehensively demonstrated that salivary gland acinar and ductal cells are robust sites for SARS-CoV-2 infection and replication, eliciting local immune cell activation. Moreover, the authors demonstrated that saliva from acutely infected patients could infect and replicate in Vero cells, *ex vivo*, indicating that the source of virus in saliva is likely derived from infected cells in the salivary glands[9]. In fact, clinical observations are in support of SARS-CoV-2 mediated damage to the salivary glands as COVID-19 patients frequently present with gustatory dysfunction and xerostomia, and cases of inflamed salivary glands have been reported in this population[10,11.]

We performed mechanistic and clinical studies to demonstrate that SARS-CoV-2 infection of salivary gland tissue compromises histatin-5 production favoring *C. albicans* proliferation, potentially predisposing infected individuals to oral candidiasis. First, we examined RNA sequencing data from infected and control parotid glands and showed significantly reduced expression of histatin genes (*HTN1,* p=0.0022*; HTN3,* p=0.0038; Supp.Fig.1a). To confirm*, in situ* hybridization and immunofluorescence co-localization studies of SARS-CoV-2 and histatins, respectively, demonstrated significant ($p<0.001$) reduction of histatin in virus infected acinar cells in parotid gland tissue obtained from deceased COVID-19 patients; further histatin intensity was inversely proportional to viral count (Fig.1a-e, Supp.Fig.1b,c). Clinical studies were conducted using two COVID-19 patient cohorts (hospitalized and outpatient), with ranging disease severity and matched healthy controls. Using an immunoassay to measure salivary histatin-5 concentrations, significant (p=0.0303) differences in values were seen where the average concentrations for the control group (n=26) was 21.3 µg/ml (11.1 µg/ml-34.5 µg/ml) and for the COVID-19 group (n=26), 18.4 µg/ml (1.4 µg/ml-53.5 µg/ml). Strikingly, 14 of the COVID-19 patients had concentrations below 10 µg/ml (Fig.1f), and although unclear why, 3 subjects had concentrations higher than any of the controls. The difference in concentrations between the two groups was also seen in age- and race-matched comparison between COVID-19 patients and control subject (Fig.1g). *Candida* colonization was assessed by culturing samples; where no *Candida* was recovered from any of the healthy controls, 45% (9/20) of COVID-19 patients sampled were positive for *C. albicans* (Fig.1f). Of note, the 3 COVID-19 patients with exceptionally high histatin-5 were positive for *C. albicans,* potentially indicating a spike in response to *C. albicans*. The findings from the hospitalized cohort were in line with those from a prospectively sampled outpatient COVID-19 cohort where histatin-5 concentrations were also significantly ($p<0.0001$) lower, compared to a control

group (Supp.Fig.2a). Prospective analysis of serial samples from these subjects indicated a trend in increase in histatin-5 concentration from the post-acute to the chronic phase (Supp.Fig.2b).

In addition to these cohorts, two subjects with mild-to-moderate COVID-19 were longitudinally sampled during their COVID-19 disease up to 39 and 80 days, respectively. For these subjects, salivary histatin-5 concentrations were measured prior to COVID-19 infection (Fig.2a, Supp.Fig.3). Compared to their pre-COVID-19 concentrations, the first saliva sample collected after COVID-19 infection, histatin-5 was 52.23% (32.8 vs 15.65 µg/ml) and 64.33% (15.7 vs. 5.6 µg/ml) lower, respectively. In both subjects, histatin-5 increased, peaking on days 15 and 45, respectively, before returning to pre-COVID-19 levels on last day sampled. Significantly, for one of the subjects, *C. albicans* was recovered from the initial samples, but not from the samples that followed the restoration of histatin-5. Three additional subjects (subjects 3, 4, and 5) were monitored prospectively over their COVID-19 disease (Supp.Fig.4). Although pre-COVID-19 saliva was not available for this group, the trend in changes in histatin-5 were comparable to subjects 1 and 2, where histatin-5 was lowest in the first samples recovered during acute phase of disease (2.4, 4.1 and 5.6 µg/ml, respectively) and increased during the post-acute phase (10.9, 13.2, and 12.5 µg/ml, respectively) in the last samples tested (Supp.Fig.4). Collectively, these findings indicate that the decrease in histatin-5 during COVID-19 is likely reversible; however, based on the observed inversely proportional association between histatin and viral counts in infected acinar cells (Fig.1a-e), in severe COVID-19, the damage may be irreparable, and affected individuals may remain predisposed to oral candidiasis as part of the Long COVID syndrome[12] (https://www.covid.gov/be-informed/longcovid/about#term).

Antimicrobial peptides, including histatins, are part of the host Th17-type adaptive immune response[8]. Interleukin-17 (IL-17) is a pro-inflammatory cytokine that regulates multiple immune events[13]. In the tissues of the oral cavity, including the salivary glands, the IL-17/Th17 signaling pathway is essential for host protection against *C. albicans* infection[13,14]. Cytokine profiling performed on saliva samples from subjects 1 and 2 demonstrated a similar trend to histatin-5, where compared to pre-COVID-19 samples, a notable increase in the Th17 associated inflammatory cytokines was observed (Supp.Fig.3). In both subjects, maximal concentrations were detected during the post-acute phase, and decreased over the subsequent days to baseline levels. Interestingly, in both subjects, the spike in cytokine concentrations coincided with salivary histatin-5 recovery, and the clearance of *C. albicans* in subject 2 (Fig.2a). The activation of the Th17 immune response is expected as immunophenotyping and microscopic analysis of demonstrated chronic, focal lymphocytic sialadenitis with a T-lymphocytic infiltrates in SARS-CoV-2 infected salivary glands[9,11]. As IL-17 antifungal activity involves regulation of the expression of antimicrobial peptides, including histatins[8,13,14], the gradual increase in histatin-5, concomitant with clearance of *C. albicans* may also be mediated by activation of Th17 response.

The importance of salivary histatin-5 in controlling the proliferation of *C. albicans* was demonstrated using an *ex vivo* anti-candidal assay. Saliva recovered from subjects (n=3) during acute COVID-19 infection (low histatin-5) and post-acute recovery (high histatin-5) phases were separately pooled, and histatin-5 concentrations measured, and subsequently tested *in vitro* for the ability to inhibit *C. albicans* proliferation (Fig.2b). Pooled saliva samples obtained during acute COVID-19 and post-recovery had average histatin-5 concentrations of 0.5 µg/ml and 11.5 µg/ml, respectively. Following *in vitro* inoculation of saliva with *C. albicans*, an average of 2.55×10^4 cells/ml *C. albicans* was recovered from the low histatin-5 sample, and 1.29×10^4 cells/ml from the high, indicating that COVID-19 low histatin-5 saliva allowed *C. albicans* to proliferate significantly (Fig.2c,d). These findings provide experimental evidence establishing the importance of salivary histatin-5 in preventing *Candida* infestation by maintaining colonizing *Candida* in the commensal state, as we previously showed in rodent models of oral candidiasis[15-17]. Collectively, these results underscore the oral cavities' diverse susceptibilities to SARS-CoV-2 infection, prompting a reassessment of oral opportunistic infection risks and their potential long-term impacts on oral health.

METHODS

Co-localization of SARS-CoV-2 and histatin in salivary gland tissue using *in situ* hybridization and immunofluorescence, respectively. To investigate the expression of histatin during SARS-CoV-2 infection, we employed the RNAscope Multiplex Fluorescent v2 assay with antigen co-detection, adhering to the manufacturer guidelines. Studies were performed on parotid FFPE (formalin-fixed, paraffin-embedded) biopsies from uninfected donors (n=4) and from COVID-19 subjects (n=8) at autopsy with high and low copy virus number. Uninfected donors were procured from the Human Cooperative Tissue Network, and COVID-19 autopsy tissues were procured by the NIH COVID-19 Autopsy Consortium as described previously[9,18]. Initially, slides were dried in an air oven at 60°C for 30 min and subsequently rehydrated, and target retrieval was performed using 1X Co-Detection Target Retrieval for 20 min at 99°C. Slides were then rinsed briefly in water and washed in PBS-T (1X PBS, 0.1% Tween-20, pH 7.2), and a hydrophobic barrier was established using an ImmEdge pen. Primary antibodies against histatin-3 (Biorbyt; diluted 1:300 in Co-detection Antibody Diluent from ACD) and AQP5 (SantaCruz; diluted 1:300 in Co-detection Antibody Diluent from ACD) were applied and slides were incubated overnight at 4°C. Following washing in PBS-T, tissues and antibodies were fixed in 10% Neutral Buffered Formalin (NBF) for 30 min at room temperature, followed by another wash in PBS-T. Tissue sections were then treated with RNAscope Protease Plus for 30 min at 40°C and immediately followed by probe hybridization using either a positive control probe (320861), negative control probe (320871), or the V-nCoV2019-S probe (848561). The V-nCoV2019-S probe is antisense and specifically targets the spike protein sequence of viral RNA, providing insights into infection and viral load within the tissue. Following hybridization, signals were amplified and visualized using fluorescence Tyramine signal amplification. The primary antibodies were detected using secondary antibodies conjugated to AF488 (histatin-3), and AF568 (AQP5; aquaporin-5) and counterstaining was performed with DAPI. Images were captured using a Zeiss Axio Scan Z1 slide scanner light microscope equipped with a 40x/0.95 N.A. objective, and image files were imported into Visiopharm software version 2017.2. We first segmented the cells using the AI app from Visiopharm, once the cells were segmented, using the APP Author function we designed an algorithm that detects the dots of ISH and counts the number of dots per cell, and quantify the mean intensity of histatin-3 per cell. The data was exported and analyzed in Prism 10.

Bulk RNAseq analysis of salivary gland tissue. Total RNA was extracted from RNAlater (Invitrogen)-preserved parotid gland at autopsy from uninfected donors (n=3) and COVID-19 subjects (n=8), using the RNeasy Mini (Qiagen) according to manufacturer protocols. Following standard bulk RNAseq using Illumina platform, normalized counts per million (CPM) were plotted for *HTN1* and *HTN3* and expression levels of both genes were compared.

Study subjects. <u>*Hospitalized cohort.*</u> Adult COVID-19 patients (n=26) hospitalized at the University of Maryland Medical Center and a matched control (age, race and gender) group of healthy volunteers (n=26) were enrolled in the study. The University of Maryland Baltimore Institutional Review Board approved this study, no patient identifiers were used and informed consent was obtained from all subjects. Inclusion criteria for control subjects included: healthy adults over 18 years of age with no history of oral candidiasis, any predisposing factors or antifungal therapy. As the premise of the study is to investigate the presence of the virus in the oral cavity regardless or disease severity, the only inclusion criteria for the COVID-19 cohort was COVID-19 positivity regardless of other factors. The COVID-19 population included 14 males and 12 females; 15 Caucasians and 11 African American with age range of 29-76. <u>*Outpatient cohort.*</u> 68 prospectively collected samples from 33 subjects at NIDCR. <u>*Prospective cases.*</u> In addition to the cohorts, 5 otherwise healthy outpatient subjects (4 females, one male; age range 30-58) were prospectively sampled at different timepoints during the course of their COVID-19 disease. A total of 29 samples were collected and analyzed for these subjects. Timeline of sampling and analysis are outlined in Fig. 2a and Supp Fig. 4.

Clinical Samples. Saliva samples were collected from all participating subjects using the Salivette collection system as we previously performed[19,20]. Saliva was recovered, aliquoted and immediately stored at -80°C with protease inhibitors. In addition, oral swabs of the oral mucosal tissue were recovered for culturing to evaluate *Candida* recovery. Due to inaccessibility to patients due to medical status, samples for fungal culturing were only obtained from 20 of the 26 hospitalized patients. For the outpatient cohort, whole unstimulated saliva samples were collected.

Evaluation of salivary *Candida* colonization. Oral swabs from all sampled subjects were immediately cultured on fungal Yeast Peptone Dextrose (YPD) agar media (Difco Laboratories) and incubated at 35°C for 24-48 h for fungal growth evaluation. The chromogenic medium CHROMagar Candida was used for *Candida* speciation.

Measurement of histatin-5 (Hst-5) salivary levels using ELISA. ELISA was performed as we previously described[9] A high purity Hst-5 peptide was synthesized by GenScript and Hst-5 specific rabbit polyclonal antibody was produced by Lampire Biological Laboratories. For measurement of Hst-5 levels, a standard curve was performed with each assay using Hst-5 peptide concentrations ranging from 0.5-500 µg/ml. Wells of high-binding 96-well plates were coated with 100 µl of each Hst-5 concentration or 1/100 dilution of saliva. Following overnight incubation at 4°C, wells were blocked with 0.1% dry milk in PBS for 1 h and anti-Hst-5 antibody (1/1000) (100 µl) was added for 1 h at 37°C. Following washing, HRP-labeled goat anti-rabbit secondary antibody (1/3000) (Abcam) was added, and plates incubated for 1 h at 37°C. Following washing, 100 µl of ABTS Peroxidase Substrate (KPL, Inc.) was added and plates incubated for 20 min until color develops. The reaction was stopped by the addition of 50 µl of Stop Solution (KPL, Inc.) and optical density (OD) was measured at 405nm using a microtiter plate reader. A standard curve was plotted with each run; samples were tested in triplicate on two separate occasions and the average Hst-5 concentration calculated in µg/ml. As there are no set normal Hst-5 salivary concentrations, based on our experience with clinical studies on Hst-5 salivary levels using our immunoassay, arbitrary concentrations of approximately 9-10 µg/ml was considered the cutoff whereby lower concentrations are considered in the low range[19].

Salivary cytokines profiling. Saliva samples from outpatient subjects were analyzed at the University of Maryland Cytokine Core using the Luminex Multianalyte System. Each sample was measured in triplicate and results expressed in Pg/ml. For the hospitalized cohort, not enough saliva was available for cytokine analysis.

***Ex vivo* salivary *C. albicans* inhibition assay.** In order to assess the anti-candidal potency of saliva with respect to Hst-5 concentration, saliva samples were recovered from 3 subjects during COVID-19 and after recovery, then pooled to generate a COVID-19 positive and a COVID-19 negative sample. Hst-5 concentration was pre-determined by ELISA and samples were filter-sterilized and comparatively tested for efficacy in inhibiting *C. albicans* proliferation *in vitro*. For these assays, cultures of the standard *C. albicans* SC5314 strain were grown in YPD broth (Difco Laboratories) overnight at 30°C with shaking and cells were washed and resuspended in sterile PBS (1mM). *C. albicans* cells were added to each of the saliva samples (100 µl) at final cell density of 1×10^4 cells/ml in the wells of a 96-well microtiter plate and plates were incubated for 1 h at 37°C with shaking. Aliquots from reactions were diluted with PBS and plated on YPD agar and incubated for 24–48 h at 35°C. The number of single colonies on each plate was counted and growth inhibition was determined based on CFU counts (cells/ml).

Statistical analysis. Statistical analysis was performed using GraphPad Prism 10.2.1. A Wilcoxon rank-sum test was used to compare Hst-5 levels between COVID-19 patients and healthy control subjects. For *in vitro* assays, Hst-5 levels in pooled saliva of COVID-19 positive and negative subjects and *Candida* CFU counts were determined using the unpaired two-sample t-tests. Significance of *HTN1* and *HTN3* expression levels in parotid glands was determined using ANOVA analysis with Bonferroni correction for multiple measurement. Figures were constructed using GraphPad Prism 10.2.1 and R statistical programming software.

ACKNOWLEDGMENT. We would like to acknowledge the contributions of the clinical coordinators LaToya Stubbs and Kendra Petrick who organized sampling of hospitalized cohort at the University of Maryland Medical Center. We would like to thank the NIH COVID-19 Autopsy Consortium (PIs-Chertow & Kleiner) for coordination and access to tissues from fatal COVID-19 cases. We give our special thanks to the members of the NIDCR Sjögren's Disease Clinical Research Team for their coordination of patients and collection of research data and tissues. Biorender.com was used to create elements of figures.

FUNDING. This work was funded by the National Institutes of Health (NIH), National Institute of Dental and Craniofacial Research (NIDCR), Division of Extramural Research (R21-DE031888, PI-Rizk-Jabra, Co-I-Warner). This project was also funded by the University of Maryland Baltimore, Institute for Clinical & Translational Research (ICTR) (1UL-1TR00309, PIs-M.A.J-R & P.R). Funding was also provided through the Intramural Research Programs of the NIH/NIDCR (Z01-DE000704, PI-Warner), NIH Clinical Center, and the National Institute of Allergy and Infectious Diseases (ZIA CL090070-03, PI-Chertow). This research was supported in part by the NIDCR Genomics and Computational Biology Core: ZIC DC000086.

AUTHOR CONTRIBUTIONS. M.A.J-R., B.M.W., A.S., T.F.M., P.R. conceived and designed this research, M.A.J-R., B.M.W. provided funding; A.A.A., T.W.W., P.P., B.M.W. performed the experiments; D.E.K, D.S.C., S.M.H., B.G., S.S., S.R., collected and processed tissues and clinical data for COVID-19 autopsies; D.E.K, S.M.H., B.G., performed the autopsies; D.S.C. and D.E.K., led and oversaw the NIH COVID-19 Autopsy Consortium; M.A.J-R., A.A.A., T.W.W., P.P., B.M.W., A.S., T.F.M., analyzed data; M.A.J-R., A.A.A., T.W.W., B.M.W. wrote the paper; B.M.W. led and oversaw the execution of NIH clinical and molecular studies supporting this work; M.A.J-R. oversaw the entire study.

ETHICAL APPROVAL. *NIH.* Autopsies are exempt from NIH single institutional review board (IRB), consent from families of fatal COVID-19 cases were obtained. Otherwise, NIH single IRB conducts ethical reviews for human research studies as required by Department of Health and Human Services regulations for the Protection of Human Subjects. All patients seen at the author's (B.M.W.) institute (NIH/NIDCR) reported herein provided informed consent before participation in IRB-approved research protocols (NIH IRB: 20-D-0094, NCT04348240; NIH IRB: 15-D-0051, NCT02327884). Individuals on 20-D-0094 had the option to receive a $50 payment per visit ($300 total) to offset the cost of travel.

REFERENCES

1 Amorim Dos Santos, J. *et al.* Oral manifestations in patients with COVID-19: A living systematic review. *Dent Res* **100**, 141-154 (2021).

2 Vila, T., Rizk, A. M., Sultan, A. S. & Jabra-Rizk, M. A. The power of saliva: Antimicrobial and beyond. *Plos Pathog* **15,** e1008058 (2019).

3 Oppenheim, F. G. *et al.* Histatins, a novel family of histidine-rich proteins in human parotid secretion. *J Biol Chem* **263**, 7472-7477 (1988).

4 Ahmad, M., Piludu, M., Oppenheim, F. G., Helmerhorst, E. J. & Hand, A. R. Immunocytochemical localization of histatins in human salivary glands. *J Histochem Cytochem* **52**, 361-370 (2004).

5 Edgerton, M. *et al.* Candidacidal activity of salivary histatins. *J Biol Chem.* **272**, 20438-20447 (1998).

6 Jabra-Rizk, M. A. *et al. Candida albicans* pathogenesis: Fitting within the host-microbe damage response framework. *Infect Immun* **84**, 2724-2739 (2016).

7 Vila, T., Sultan, A. S., Montelongo-Jauregui, D. & Jabra-Rizk, M. A. Oral candidiasis: A disease of opportunity. *J Fungi (Basel)* **6**, 15 (2020).

8 Salvatori, O., Puri, S., Tati, S. & Edgerton, M. Innate immunity and saliva in *Candida albicans*-mediated oral diseases. *J Dent Res* **95**, 365-371 (2016).

9 Huang, N., Pérez, P., Kato, T. & al., e. SARS-CoV-2 infection of the oral cavity and saliva. *Nat Med* **27**, 892-903 (2021).

10 Corchuelo, J. & Ulloa, F. C. Oral manifestations in a patient with a history of asymptomatic COVID-19: Case report. *Int J Infect Dis.* **100**, 154-157 (2020).

11 Shen, Y. *et al.* Evidence of a Sjögren's disease-like phenotype following COVID-19 in mice and humans. *JCI Insight* **8**, e166540 (2023).

12 Pisano, M. *et al.* Oral candidiasis in adult and pediatric patients with COVID-19. *Biomedicines* **11**, 846 (2023).

13 Gaffen, S. L. & Moutsopoulos, N. M. Regulation of host-microbe interactions at oral mucosal barriers by type 17 immunity. *Sci Immunol* **5**, eaau4594 (2020).

14 Pavlova, A. & Sharafutdinov, I. Recognition of *Candida albicans* and role of innate type 17 immunity in oral candidiasis. *Microorganisms* **8**, 1340 (2020).

15 Kong, E. *et al.* Development and *in vivo* evaluation of a novel histatin-5 bioadhesive hydrogel formulation against oral candidiasis. *Antimicrob Agents Chemother* **60**, 881-889 (2015).

16 Sultan, A. S. *et al.* Digital design of a universal rat intraoral device for therapeutic evaluation of topical formulation against *Candida*-associated denture stomatitis. *Infect Immun* **87**, e00617-00619 (2019).

17 Sultan, A. S., Vila, T., Hefni, E., Karlsson, A. J. & Jabra-Rizk, M. A. Evaluation of the antifungal and wound healing properties of a novel peptide-based bioadhesive hydrogel formulation. *Antimicrob Agents Chemother.* **63**, e00888-00819 (2019).

18 Stein, S. R. *et al.* SARS-CoV-2 infection and persistence in the human body and brain at autopsy. *Nature* **612**, 758-763 (2022).

19 Khan, S. A., Fidel Jr , P., Al Thunayyan, A., Meiller, T. & Jabra-Rizk, M. A. Impaired histatin-5 level and salivary antimicrobial activity against *C. albicans* in HIV-infected individuals. *J AIDS Clin Res* **4**, 1-6 (2013).

20 Alfaifi, A., Sultan, A., Montelongo-Jauregui, D., Meiller, T. F. & Jabra-Rizk, M. Long-term post-COVID-19 associated oral inflammatory sequelae. *Front Cell Infect Microbiol* **12** (2022).

FIGURE LEGEND

Figure 1. Impact of SARS-CoV-2 salivary gland infection on histatin production, gene expression and salivary levels. (a-e) Co-localization studies using *in situ* hybridization for SARS-CoV-2 (*white dots* and *arrows*) and immunofluorescence for histatin-3 (*green*) with quantitative correlation between the intensity of histatin-3 and SARS-CoV-2 counts within infected acinar cells of parotid tissue from **(a)** healthy subject (*white asterisk,* non-specific signal) and **(b,d)** deceased COVID-19 patients. Acini (dotted circles) identified based on expression of AQP5 (*red,* apical membrane); *inset* (*orange box*) shows presence of viral genome in acinar cells of parotid glands. **(c,e)** Per acinar cell expression of histatin-3 and the per cell viral count are inversely proportional in two representative COVID-19 cases (p7,p19). **(f)** Histatin-5 concentrations and *C. albicans* recovery from saliva from hospitalized COVID-19 patients and matched healthy controls. **(g)** Waterfall plot depicting 26 pairs of subjects matched for race and age. Bar height represents differences among pairs in histatin-5 levels (µg/ml) between healthy controls and COVID-19 patients.

Figure 2. Prospective longitudinal sampling and analysis of saliva from two subjects with moderate COVID-19. (a) Measurement of histatin-5 concentrations and fungal culturing of samples prior to and during acute and post-acute phases of COVID-19. Line graph demonstrates a correlative trend and concomitant spike in salivary histatin-5 concentrations and IL-17F levels. **(b)** Workflow for histatin-5 quantification and proliferation assay using pooled saliva samples from 3 subjects under a COVID-19 infected state (PC+) and recovered state (PC-). **(c)** Bar plot depicts histatin-5 concentrations from pooled saliva samples. **(d)** Bar plot depicts recovered *C. albicans* CFUs (cells/ml) from pooled saliva samples seeded with $1x10^4$ cells/ml of *C. albicans*.

SUPPLEMENTAL FIGURES

Supp Fig. 1. Expression of histatin is affected by SARS-CoV-2 infection. (a) Parotid expression of histatin genes (*HTN1* and *HTN3*) from deceased COVID-19 subjects (n=8) and healthy control subjects (n=3) using bulk RNA sequencing. **(b)** Immunofluorescence (IF) and *in situ* hybridization (ISH) controls (see also Fig. 1). Positive and negative controls for IF, antibody anti-histatin-3 in control parotid shows strong IF (green) in acini structures and no signal is observed in ducts. The isotype control shows no signal. **(c)** Probe anti-human *PPIB* shows strong signal in all the cells (white); negative control probe shows sparse, rare positive signal in the tissue.

Supp Fig. 2. Salivary histatin-5 levels and fungal colonization in a prospectively sampled outpatient COVID-19 cohort and healthy controls. (a) Significant decrease in salivary histatin-5 in COVID-19 cohort compared to healthy volunteers. **(b)** Linear regression analysis represents increase in histatin-5 concentration overtime from the post-acute phase to the chronic phase, based on longitudinal samples.

Supp Fig. 3. Longitudinal prospective analysis of saliva samples from two subjects with moderate COVID-19. Changes in histatin-5 and cytokine concentrations in two longitudinally sampled subjects prior to and during the acute and post-acute phases of COVID-19 disease. Timeline of

sampling during COVID-19 disease up to 49 and 85 days for subjects 1 **(a)** and 2 **(b),** respectively. Upon culturing, *C. albicans* was recovered from samples from subject 2 **(b).**

Supp Fig. 4. Prospective longitudinal sampling and analysis of saliva from 3 subjects with moderate COVID-19. Timeline of sampling and measurement of salivary histatin-5 and cytokine concentrations in samples recovered during acute phase of the disease and upon recovery. Table presents cytokine values measured in the first and last samples recovered from the 3 subjects and the percent change in levels between the samples.

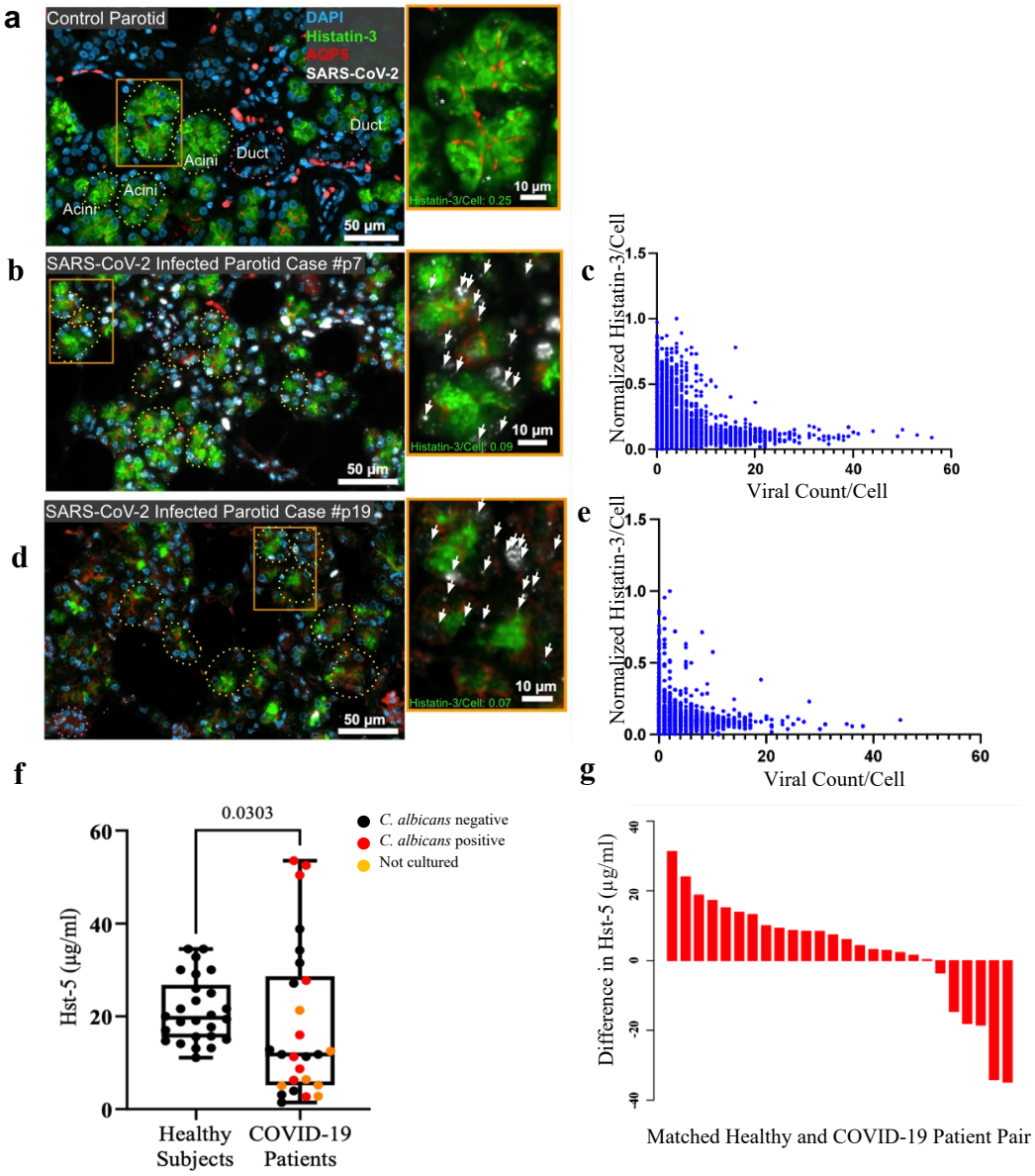

Figure 1. Impact of SARS-CoV-2 salivary gland infection on histatin production, gene expression and salivary levels. (a-e) Co-localization studies using *in situ* hybridization for SARS-CoV-2 (*white dots* and *arrows*) and immunofluorescence for histatin-3 (*green*) with quantitative correlation between the intensity of histatin-3 and SARS-CoV-2 counts within infected acinar cells of parotid tissue from **(a)** healthy subject (*white asterisk,* non-specific signal) and **(b,d)** deceased COVID-19 patients. Acini (dotted circles) identified based on expression of AQP5 (*red,* apical membrane); *inset* (*orange box*) shows presence of viral genome in acinar cells of parotid glands. **(c,e)** Per acinar cell expression of histatin-3 and the per cell viral count are inversely proportional in two representative COVID-19 cases (p7,p19). **(f)** Histatin-5 concentrations and *C. albicans* recovery from saliva from hospitalized COVID-19 patients and matched healthy controls. **(g)** Waterfall plot depicting 26 pairs of subjects matched for race and age. Bar height represents differences among pairs in histatin-5 levels (µg/ml) between healthy controls and COVID-19 patients.

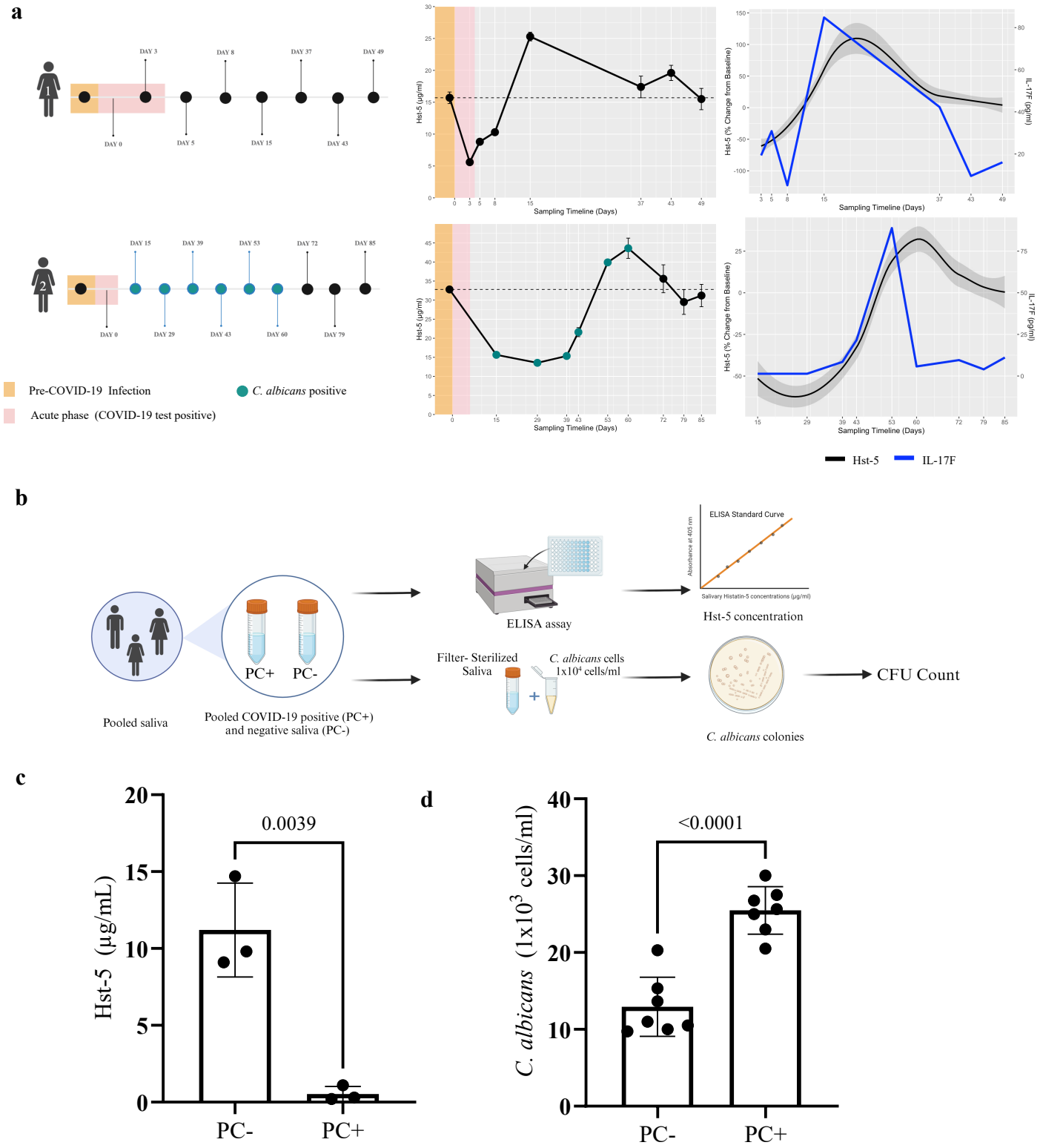

Figure 2. Prospective longitudinal sampling and analysis of saliva from two subjects with moderate COVID-19. (a) Measurement of histatin-5 concentrations and fungal culturing of samples prior to and during acute and post-acute phases of COVID-19. Line graph demonstrates a correlative trend and concomitant spike in salivary histatin-5 concentrations and IL-17F levels. **(b)** Workflow for histatin-5 quantification and proliferation assay using pooled saliva samples from 3 subjects under a COVID-19 infected state (PC+) and recovered state (PC-). **(c)** Bar plot depicts histatin-5 concentrations from pooled saliva samples. **(d)** Bar plot depicts recovered *C. albicans* CFUs (cells/ml) from pooled saliva samples seeded with $1x10^4$ cells/ml of *C. albicans*.